

# Thermal analysis of poly(2-hydroxyethyl methacrylate) (pHEMA) hydrogels

J. R. MEAKIN\*, D. W. L. HUKINS

*Department of Bio-Medical Physics and Bio-Engineering, University of Aberdeen, Foresterhill, Aberdeen AB25 2ZD, UK*

C. T. IMRIE

*Department of Chemistry, University of Aberdeen, Meston Walk, Aberdeen AB24 3UE, UK*

R. M. ASPDEN

*Department of Orthopaedic Surgery, University of Aberdeen, Polwarth Building, Foresterhill, Aberdeen AB25 2ZD, UK*

*E-mail: j.meakin@biomed.abdn.ac.uk*

The influence of water on the physical properties of a hydrogel is important for understanding natural tissues and in designing synthetic materials to replace them. In this study, poly (2-hydroxyethyl methacrylate) (pHEMA) was used as a model system to understand how water interacts with the polymer of a hydrogel. Thermal analysis methods (thermogravimetric analysis coupled to mass spectrometry and differential scanning calorimetry) were used to determine: (i) the total water content of pHEMA gels; (ii) how this water was lost during heating; (iii) the relationship between water content of the gel and its glass transition temperature; and (iv) the behavior of the water in the gel on cooling. Previous researchers have invoked various models to describe the organization of water in a hydrogel. In this study, the simplest model which could explain all of the results from the different thermal analysis techniques was one which consisted of three classes of water: (i) hydration water in close proximity to the polymer; (ii) interstitial water in regions or cavities surrounded by polymer chains; and (iii) bulk water.

© 2003 Kluwer Academic Publishers

## 1. Introduction

The study presented in this paper is part of a research program into how water in natural and synthetic hydrogels influences their physical properties. This is important in understanding how natural tissues function, and how changes in water content with aging and disease cause changes in the mechanical functions of tissues. It will also help in the design of implants to replace degenerate tissues.

As part of this work, we are interested in understanding the interactions of water with the polymer in a hydrogel. As a starting point, we chose poly(2-hydroxyethyl methacrylate), pHEMA, as a model system. There is some controversy in the literature on how water is contained in a hydrogel. Previous research has concluded that the water exists in two distinct phases; these are commonly referred to as “bound” and “free” water, but other terminology has been used [1]. Intermediate phases have also been suggested [2].

The evidence for two or more phases has been found using a variety of different methods. Differential scanning calorimetry (DSC) for example, has shown that when hydrated pHEMA is cooled and heated, not all the water in the gel either freezes or melts [2, 3]. It is this

“missing” water that has been interpreted as being “bound” to the polymer. Alternative methods have included dielectric spectroscopy [4], dilatometry [2], specific conductivity [2], nuclear magnetic resonance (NMR), [5] dynamic mechanical thermal analysis (DMTA) [6], and X-ray diffraction [7].

Despite the intuitive appeal of this model, various authors have refuted the evidence. Roorda *et al.* [8], for example, have proposed an alternative explanation for the thermal behavior in which as the pHEMA gel cools, causing the water to begin crystallizing, the gel undergoes a glass transition. This increases the viscosity of the gel, effectively preventing any further crystallization of the water. A similar interpretation of the thermal behavior of poly(ethylacrylate)/poly(hydroxyethyl acrylate) interpenetrating networks and, specifically, the tendency of water to crystallize, also invokes changes to the glass transition during cooling and heating of the gel [9]. It should be noted, however, that the latter study provided a description of the macroscopic phase diagram from a thermodynamic viewpoint and was not, therefore, a molecular interpretation of the observed behavior.

A recent review article which focuses on the evidence provided by NMR and DSC [1] shows that there is still

\*Author to whom all correspondence should be addressed.

debate on the subject, but that the two viewpoints are not completely incompatible. In this study we investigated several things: the water content of a pHEMA gel in equilibrium with water, how this water is lost when the gel is heated, how the water affects the glass transition of the gel, and what happens to the gel as it is cooled.

## 2. Materials

pHEMA was obtained from Aldrich (Aldrich Chemical Company Ltd., Milwaukee, WI, USA). Gels were prepared by soaking the dried material in excess deionized water for at least a week. The resulting gel was then placed under a weight (5 kg) for several hours to form flat discs approximately 0.5 mm in thickness. These were then stored in deionized water until required for testing.

## 3. Methods

### 3.1. Thermogravimetric analysis

Thermogravimetric analysis (TGA) was performed to determine the total quantity of water in the equilibrated gel, to determine the temperature at which the water was lost and to see if this was dependent on the heating rate. To confirm that the mass loss was due to water lost from the gel, and was not associated with decomposition of the polymer itself, the evolved gas was analyzed using a coupled mass spectrometer (Balzers ThermoStar, Balzers AG, Liechtenstein). Three samples were cut from the hydrated disks of polymer and each one hermetically sealed in a 100  $\mu\text{l}$  aluminum pan. The average mass of the samples was 8 mg (standard deviation 1 mg). Each sample was heated to 150  $^{\circ}\text{C}$  at a different rate; 1, 5, or 10  $^{\circ}\text{C min}^{-1}$ , using Mettler-Toledo equipment (TGA/SDTA 851 $^{\circ}$ , Mettler-Toledo Ltd., Leicester, UK). The experiments were performed in an inert atmosphere (either nitrogen or argon gas flowing at a rate of 200–240  $\text{cm}^3 \text{min}^{-1}$ ). The mass spectrometer was set to detect the presence of atomic mass units (amu) 17, 18, and 44 in the evolved gas. These masses were chosen as they would demonstrate the presence of water (amu 17 and 18) and carbon dioxide (amu 44).

A further five samples were heated to 150  $^{\circ}\text{C}$  at a rate of 5  $^{\circ}\text{C min}^{-1}$  and kept at this temperature for 60 min, to ensure that all the water was lost from them.

### 3.2. Glass transitions

The glass transition temperature of hydrated pHEMA was determined as a function of the water content. Samples of the completely hydrated gel were taken and dried to reduce their water content. These samples were then sealed in 0.6 ml microcentrifuge tubes for at least 48 hours to allow the sample to re-equilibrate, used for the DSC experiments and subsequently dried to constant mass to determine water content.

The thermal properties of the samples were characterized using DSC (DSC821 $^{\circ}$ , Mettler-Toledo Ltd.). The glass transition temperature was determined by heating the samples at a rate of 10  $^{\circ}\text{C min}^{-1}$ . Drier samples were heated from 25 to 150  $^{\circ}\text{C}$ . For samples with water contents such that their glass transition was near or below

25  $^{\circ}\text{C}$ , the samples were cooled to  $-15^{\circ}\text{C}$ , held at this temperature for 60 min and then reheated. To obtain the glass transition of dry pHEMA, a sample was dried in an oven at about 105  $^{\circ}\text{C}$  before testing.

After testing, a small hole was made in the lid of the DSC pan and the sample was dried for at least 24 hours in an oven at about 105  $^{\circ}\text{C}$ . The water content of the sample was thus calculated from the dry and wet masses.

### 3.3. Annealing experiments

Annealing experiments were performed to determine how much water crystallized in the gels on cooling, and if the quantity of crystallized water was dependent on annealing time. Samples of the hydrated gel were hermetically sealed in 40  $\mu\text{l}$  pans. The average mass of the samples was 10 mg (standard deviation 3 mg). A Mettler-Toledo differential scanning calorimeter (DSC821 $^{\circ}$ , Mettler-Toledo Ltd.) was used to cool the samples to either  $-25$ ,  $-50$  or  $-100^{\circ}\text{C}$  at a rate of  $-5^{\circ}\text{C min}^{-1}$ . They were then kept at this temperature for differing lengths of time up to 16 hours, and subsequently reheated at a rate of 5  $^{\circ}\text{C min}^{-1}$ . All experiments were performed in an inert atmosphere of nitrogen. The area under the freezing exotherm, the cold-crystallization exotherm (where appropriate), and the melting endotherm were measured for each annealing experiment. These areas, corresponding to the energy of the thermal events, were converted into a mass of water using the enthalpy of fusion for water (334  $\text{J g}^{-1}$  [10]). The values were then normalized by the sample mass.

## 4. Results

### 4.1. Thermogravimetric analysis

The TGA traces and mass spectra obtained for the gel sample heated at a rate of 5  $^{\circ}\text{C min}^{-1}$  are shown in Fig. 1(a)–(c). The dependence of the mass of the sample, expressed as a percentage of the initial mass, on temperature is shown in Fig. 1(a), and the first derivative of this curve in Fig. 1(b). Two distinct mass loss peaks can be seen in Fig. 1(b): a broad, weak peak centered at ca. 80  $^{\circ}\text{C}$  and a sharper, more pronounced loss at 108  $^{\circ}\text{C}$ . In addition, the higher temperature mass loss peak has a high temperature shoulder. The mass spectra for amu 17 and 18 (Fig. 1(c)) contain peaks coincident with the mass losses seen in Fig. 1(a) and 1(b) and the ratio of these peaks was consistent with this mass loss being due to water. No peaks were observed for amu 44. This implied that no thermal decomposition occurred during these experiments as this would presumably involve the evolution of carbon dioxide.

Fig. 2 shows the mass loss and mass loss rate for three different heating rates. It can be seen that on heating at the faster rate of 10  $^{\circ}\text{C min}^{-1}$  a change in slope at 113  $^{\circ}\text{C}$  is indicative of two regions of mass loss (Fig. 2(a)) while in the first derivative plot the main peak also contains some structure (Fig. 2(b)). Heating at 5  $^{\circ}\text{C min}^{-1}$  gave similar results to heating at 10  $^{\circ}\text{C min}^{-1}$ , but with the mass losses shifted to lower temperatures. Heating at the slower rate of 1  $^{\circ}\text{C min}^{-1}$ , however, resulted in only a single but rather broad mass loss being observed. For all heating rates, the mass spectra revealed that the mass loss

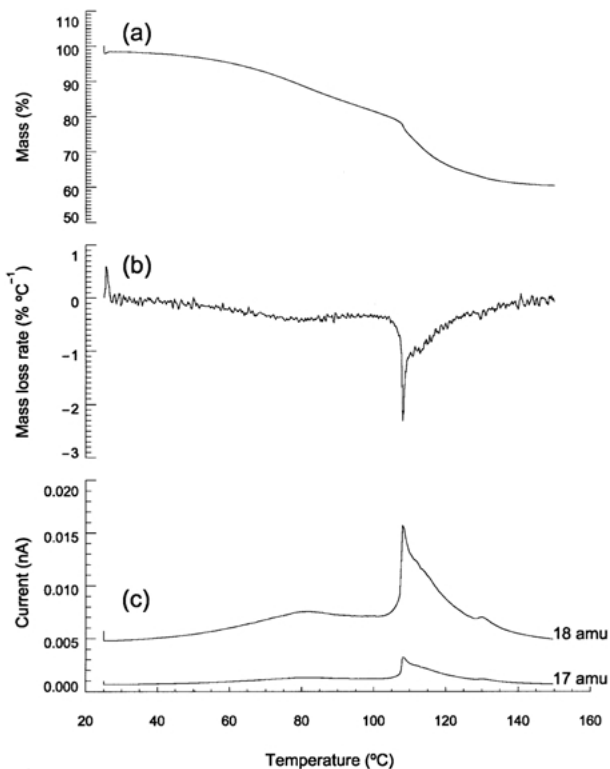


Figure 1 TGA traces and mass spectra obtained for pHEMA gel heated at a rate of  $5\text{ }^{\circ}\text{C min}^{-1}$ : (a) mass as a function of temperature (b) mass loss rate as a function of temperature (c) mass spectra for amu 17 and 18. Note: The mass is expressed as a percentage of the initial mass and the mass loss rate is calculated as the first derivative of this percentage mass with respect to temperature.

was solely due to water loss from the gel, and was not associated with decomposition of the polymer.

The samples dried for an hour at  $150\text{ }^{\circ}\text{C}$  showed that the total water content in the gels equilibrated in excess water was 43% (mean of five samples, with a standard deviation of 0%). This value for the equilibrium water content is consistent with that found by other researchers: Pedley and Tighe [3] (40%); Roorda *et al.* [8, 11] (41.2%); Fambri *et al.* [6] (38.6%). These variations presumably reflect small variations in composition.

## 4.2. Glass transitions

The DSC trace for a gel with a water content of 8% is shown in Fig. 3. This contains a step in the baseline which was assigned as a glass transition. The glass transition temperature was defined as the inflection point of the step and was determined either from the minimum of the first derivative of the curve or by using the tool available in the Mettler-Toledo STAR<sup>e</sup> software. The overshoot of the change in the heat capacity, see Fig. 3, is characteristic behavior for polymers and is most commonly attributed to an enthalpic relaxation associated with physical aging. The endothermic deflection of the baseline at high temperatures is presumably associated with the dehydration of the gel as revealed by the TGA experiments.

Fig. 4 shows the glass transition temperature of the gel as a function of water content. The glass transition temperature of dry pHEMA was found to be  $113\text{ }^{\circ}\text{C}$  and this is consistent with values reported in the literature [6, 8, 12], These data were fitted by the curve described

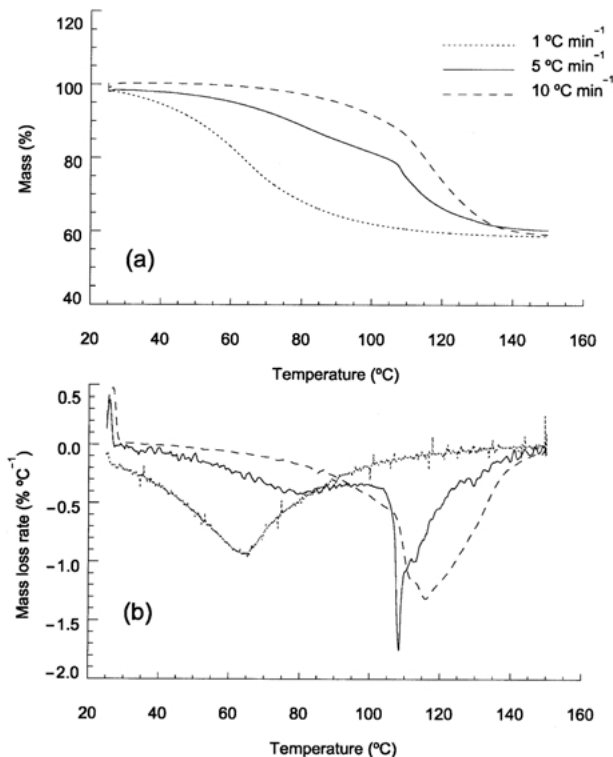


Figure 2 (a) Mass loss and (b) mass loss rate as a function of reference temperature for samples heated at  $1$ ,  $5$  or  $10\text{ }^{\circ}\text{C min}^{-1}$ . The mass is expressed as a percentage of the initial mass and the mass loss rate is calculated as the first derivative of this percentage mass with respect to temperature.

by Equation 1 using IDL software (Interactive Data Language version 5.3, Research Systems Inc., Boulder, Colorado, USA):

$$\frac{100}{T_g(\text{gel})} = \frac{W}{T_g(\text{water})} + \frac{(100 - W)}{T_g(\text{pHEMA})} \quad (1)$$

where  $T_g(\text{gel})$  is the glass transition temperature of the gel,  $T_g(\text{water})$  that of water and  $T_g(\text{pHEMA})$  that of the dry polymer, measured here to be  $386\text{ K}$ , and  $W$  is the total water content of the gel (%). As there is a spread of values in the literature for the glass transition of water,  $T_g(\text{water})$  was left unfixed. Equation 1 is known as the Fox equation and is suitable for polymers containing low

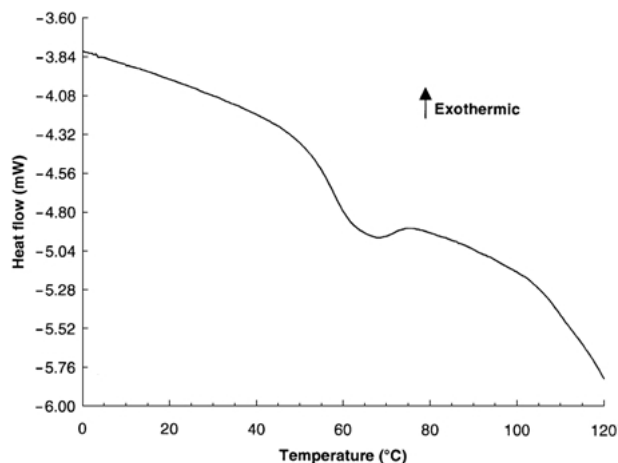


Figure 3 DSC trace obtained on heating for a pHEMA gel with 8% water content. The glass transition temperature was defined as the inflection point of the step in the baseline.

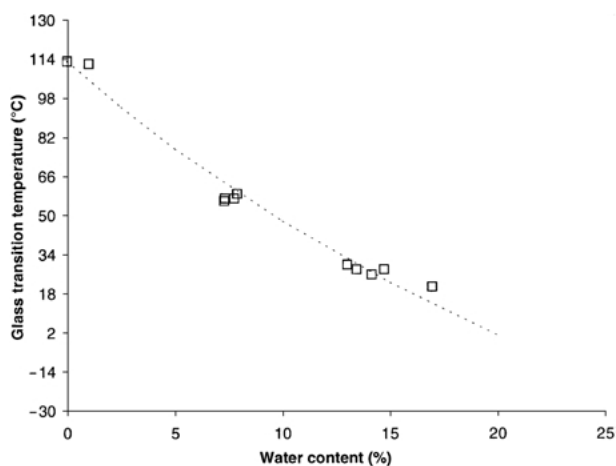


Figure 4 Glass transition temperature of the gel as a function of water content. The water content is expressed as the percentage of the total sample mass. The curve (dotted line) was fitted using Equation 1.

molar mass plasticizers such as water [13]. Other researchers, however, have used alternative models [12]. The fitted curve is also shown in Fig. 4 and the correlation coefficient of the fit was 0.9899. The glass transition temperature of water was predicted by the curve fitting to be  $-146^{\circ}\text{C}$  and this is consistent with values in the literature [14]. Thus, the application of the Fox equation to fit the data appears reasonable.

### 4.3. Annealing experiments

The DSC traces measured on cooling to the annealing temperature and on the subsequent heating cycle are shown in Figs. 5 and 6, respectively. Each set of cooling traces contains an irregularly shaped set of peaks between ca.  $-15$  and  $-25^{\circ}\text{C}$ . The onset temperature

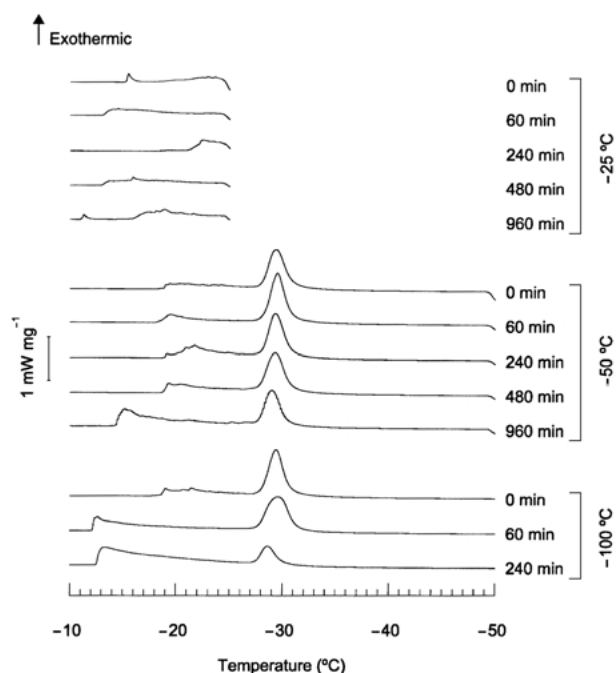


Figure 5 DSC traces of pHEMA obtained on cooling to  $-25$ ,  $-50$  or  $-100^{\circ}\text{C}$  at a rate of  $5^{\circ}\text{C min}^{-1}$ . Annotations refer to the length of the anneal time after this cooling ramp. A scale bar shows the heat flow normalized by the sample mass.

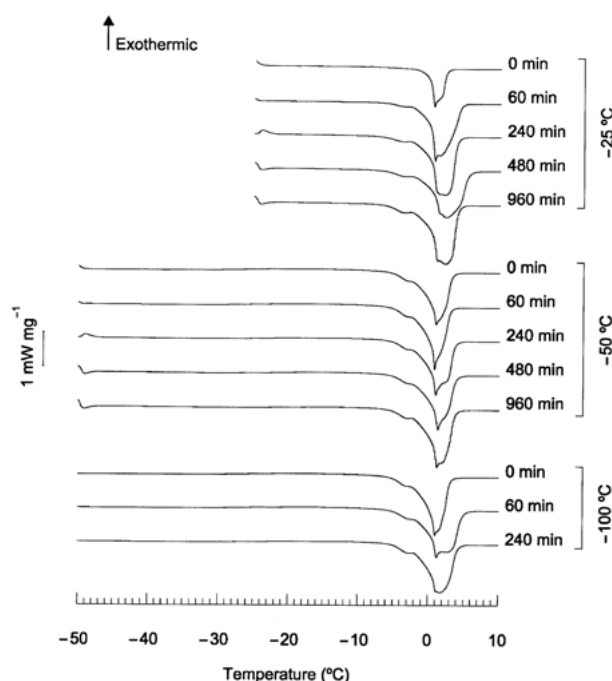


Figure 6 Thermograms of pHEMA heated from  $-25$ ,  $-50$  or  $-100^{\circ}\text{C}$  at a rate of  $5^{\circ}\text{C min}^{-1}$ . Annotations refer to the length of the anneal time before this heating ramp. A scale bar shows the heat flow normalized by the sample mass.

and profile of these peaks are highly irreproducible, see Fig. 5. This collection of peaks is presumably associated with the crystallization of supercooled water. The irregularity of these peaks was also referred to by Roorda *et al.* [11] and we will discuss this later. By contrast, on cooling to either  $-50$  or  $-100^{\circ}\text{C}$  each trace contains a well-defined peak with an onset temperature of  $-27^{\circ}\text{C}$  and a peak at ca.  $-30^{\circ}\text{C}$ . The enthalpies associated with these two transition regions, i.e. ca.  $-15$  to  $-25^{\circ}\text{C}$  and ca.  $-30^{\circ}\text{C}$ , are clearly inter-related, see Fig. 5. Thus, the larger the enthalpy associated with the first region, the smaller that of the second event. Quantifying this is not possible as the two regions overlap and the baseline does not return to its original value until the second event is complete. On cooling to  $-25^{\circ}\text{C}$  only the first exothermic event is evident in the DSC traces.

The DSC traces obtained on reheating the gels are shown in Fig. 6. For the gels annealed at  $-50$  or  $-100^{\circ}\text{C}$ , a small exotherm was observed just prior to the onset of melting (starting between  $-46$  and  $-27^{\circ}\text{C}$ ) which is not apparent, however, on the scale used in Fig. 6. This is presumably associated with the cold-crystallization of a small quantity of water which did not crystallize on cooling or annealing. This exotherm was not present in the DSC traces of the gels annealed at  $-25^{\circ}\text{C}$ . The endotherms associated with the melting transition are broad, consisting of at least three overlapping peaks. The central peak is at ca.  $1^{\circ}\text{C}$  and this has both lower and higher temperature shoulders.

The mass of water (expressed as a fraction of sample mass) that crystallized, cold-crystallized (where appropriate), and melted is given for each experiment in Table I. We must stress, however, that these values are calculated using the enthalpy of fusion of pure water and assuming that pure water is involved in each of these

TABLE I Mass of water that crystallized, cold-crystallized and melted in each sample calculated using the enthalpy associated with each event. Also given is the ratio of total detected frozen water to that measured during melting

Annealing temperature (°C)	Annealing time (min)	Crystallized water (mg/g/gel)	Cold-crystallized water (mg/g gel)	Melted water (mg/g gel)	Ratio of crystallized water to melted water	Unfrozen water (mg/g gel)	Unfrozen water (mol/monomol pHEMA)
-25	0	20	N/A	69	0.30	361	4.6
-25	60	33	N/A	205	0.16	225	2.8
-25	240	21	N/A	228	0.09	202	2.6
-25	480	38	N/A	236	0.16	194	2.5
-25	960	43	N/A	246	0.18	184	2.3
-50	0	87	20	178	0.60	252	3.2
-50	60	98	18	185	0.63	245	3.1
-50	240	107	8	196	0.59	234	3.0
-50	480	107	11	196	0.60	234	3.0
-50	960	123	7	211	0.62	219	2.8
-100	0	99	18	190	0.62	240	3.0
-100	60	130	17	218	0.67	212	2.7
-100	240	127	13	208	0.67	222	2.8

transitions. This assumption while not strictly valid does provide a good first order approximation of the mass of water melting [9]. Fig. 7 shows the crystallized and melted water as a function of annealing time. It can be seen from Fig. 7 that the mass of water that melted on heating for samples annealed at  $-25^{\circ}\text{C}$  increased considerably with annealing time, especially in the first one to two hours of annealing. These results are consistent with those found by Roorda *et al.* [11]. By contrast, the quantity of water that melted on heating after annealing at  $-50$  or  $-100^{\circ}\text{C}$  had a much weaker dependence on annealing time although the masses of both crystallized and melted water do increase with annealing time. It is particularly apparent in Fig. 7 that in every sample the amount of water detected on melting is significantly greater than that estimated from the crystallization behavior. Table I lists the ratios of crystallized water to melted water. This ratio is lowest for the annealing temperature of  $-25$  and greatest for  $-100^{\circ}\text{C}$ . The largest value observed is 0.68 after 240 min annealing at  $-100^{\circ}\text{C}$ . We will return to this observation later.

In each sample a given amount of water is unaccounted for in the melting process and this is listed in Table I both in terms of its mass expressed as a fraction of the sample mass and as a ratio of the number

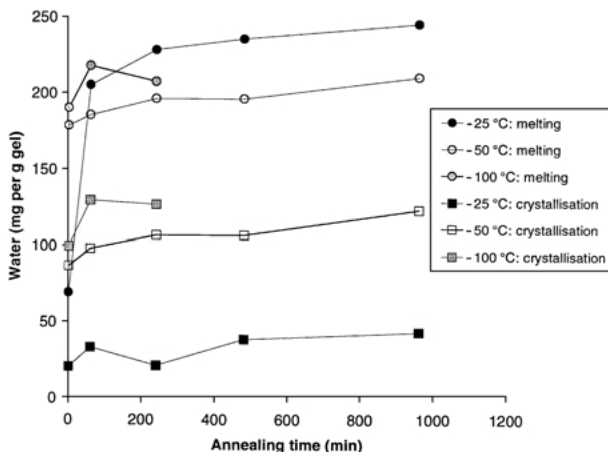


Figure 7 Normalized mass of water crystallizing or melting as a function of annealing time.

of moles of water per pHEMA repeat unit. The proportion of this non-crystallizable water shows a stronger dependence on annealing time at  $-25^{\circ}\text{C}$  than at either  $-50$  or  $-100^{\circ}\text{C}$ , although it tends to decrease with time at all three temperatures.

## 5. Discussion

The simplest model with which to account for the thermal behavior of water in hydrogels allows for just one type of water [9, 11]. Within this framework a single mass loss would be expected on increasing temperature and this is indeed observed in the TGA trace obtained at  $1^{\circ}\text{min}^{-1}$ , see Fig. 2. The TGA traces measured at faster heating rates, however, clearly show multiple mass losses. This may imply that, at the faster heating rates, an appreciable temperature gradient is established across the sample. We consider this explanation to be unlikely given the large differences in temperature between the mass losses, see Fig. 2. An alternative explanation invokes a phase transition within the sample on losing a given amount of water. Thus, as water is lost the glass transition of the hydrogel increases, see Fig. 4, and at some point the glass transition temperature exceeds that of the furnace. It is quite feasible that water loss would now be kinetically inhibited. This reduces the rate at which  $T_g$  increases and so the furnace temperature can now exceed  $T_g$  and water loss is accelerated. This would continue until the gel was dehydrated and have the appearance of multiple mass losses. The maximum  $T_g$  for this system, however, is that of dehydrated pHEMA which, as we have seen, is  $113^{\circ}\text{C}$  but water loss continues to much higher temperatures and in a nonmonotonical fashion. It is difficult, therefore, to account for the TGA data of the hydrogels in terms of a model in which all water is indistinguishable.

If we now consider the DSC data obtained for these hydrogels, see Figs. 5 and 6, then there are a number of features which must be accounted for. On cooling, crystallization occurs over a very wide temperature range and consists of an irregular series of peaks and a well-defined event at ca.  $-30^{\circ}\text{C}$ . Within the framework of having just a single type of water, this behavior is difficult to interpret although it has been suggested that

the first region of crystallization is that of water trapped in cavities within the gel and hence is not homogeneously mixed with the polymer [9]. The exotherm at ca.  $-30^{\circ}\text{C}$  is thought to be associated with the crystallization of the water homogeneously mixed with the polymer chains. The broad melting endotherm is also thought to reflect the presence of these two types of water. Thus, even the proponents of energetically indistinguishable water need to invoke two types of water to account for the crystallization behavior of water within the hydrogel [9].

It is clear, therefore, that the thermal behavior of pHEMA hydrogels simply cannot be accounted for within the framework of a model in which all the water is energetically indistinguishable. Thus, we must now increase the complexity of the model and introduce different types of water within the hydrogel. Specifically, we invoke three classes of water: (i) hydration water which is in close proximity to the polymer and which does not freeze in these experiments; (ii) interstitial water in regions or cavities surrounded by polymer chains; (iii) bulk water. This model is essentially that proposed elsewhere to interpret, for example, the Raman spectra of hydrogels [15] and is analogous to that used to account for the freezing behavior of water confined in multilamellar phospholipids [16]. Within type (i), there will exist energetically different types of water arising from the amphiphilic nature of the polymer. For example, there will be an enhancement of the hydrogen bonding between water molecules in hydration shells surrounding hydrophobic segments of the polymer chains, i.e. on average each water molecule will participate in a larger number of hydrogen bonds than a water molecule in bulk water. By contrast, the hydration water surrounding hydrophilic segments will have a structure more similar to that of bulk water. These differing hydration shells will coexist. The second class of water arises from structural heterogeneity within the gel. Chain entanglements and inter- and intramolecular hydrogen bonding between polymer chains give rise to cavities. These cavities may either be hydrophilic or hydrophobic in nature which again will influence the structure of water contained within them. This effect will depend on the size of the cavity in question. Finally, there will exist water whose structure and hence thermal behavior will be essentially identical to that of bulk water. It is important to note that these differing classes of water will coexist in dynamic equilibrium and that the energy differences between them are likely to be very small.

If we now return to the TGA data shown in Figs. 1 and 2, of the faster heating rates, the multiple mass losses can now be assigned to energetically different types of water. The single mass loss at the slowest heating rate which at first sight does not support this view, may instead indicate that at high temperatures and slow heating rates the energy differences between the types of water are so small that they are no longer kinetically distinguishable. Thus, the dynamic equilibrium is maintained throughout the experiment and dehydration occurs as a single process. This accounts also for the rather broad mass loss observed. By contrast, at the faster heating rates this equilibrium is not preserved and multiple mass losses are observed. At lower temperatures the equilibria will respond more slowly to changes in composition and in

principle it should be easier to freeze in non-equilibrium arrangements. This view is supported by the DSC traces shown in Figs. 5 and 6. Thus, the crystallization of water trapped in cavities will occur first on cooling but the freezing temperature will depend on both the nature and size of the cavity. Each sample will have a different microstructure and thus this initial crystallization will vary from sample to sample and be rather complex. At lower temperatures the bulk water spontaneously crystallizes over a relatively narrow temperature range, consistent with the homonucleation model [17], and is seen at ca.  $-30^{\circ}\text{C}$  in Fig. 5. The quantity of water which freezes during these processes will depend on the microstructure of the gel but clearly the more water trapped in cavities the less will freeze at ca.  $-30^{\circ}\text{C}$  and vice versa. Again, such a relationship between the freezing enthalpies is clearly seen in Fig. 5. On heating, the interstitial and bulk water would be expected to show differing melting points and this accounts for the rather broad melting endotherms seen in Fig. 6. The non-crystallizable water, see Table I, represents hydration water surrounding both hydrophilic and hydrophobic polymer segments.

There remains one aspect of the DSC data still to be accounted for and that is the discrepancy between the mass of water measured during melting and that during crystallization, see Table I and Fig. 7. The data measured on cooling for samples annealed at  $-25^{\circ}\text{C}$  are unreliable because the baseline has not returned to its original value making a meaningful area measurement impossible, see Fig. 5. By contrast, on cooling to either  $-50$  or  $-100^{\circ}\text{C}$  the baseline has returned to a steady value and an accurate area measurement of the freezing region is apparently possible. We must remember, however, that, on cooling, the gel will undergo a glass transition at a temperature which may be estimated using Equation 1. Thus if we assume that all the unfrozen water, see Table I, is acting as a plasticizer then for the samples cooled to  $-50^{\circ}\text{C}$ ,  $T_g$  will vary between  $-48$  and  $-55^{\circ}\text{C}$  and these would not be detected in the DSC experiments. However, on cooling to  $-100^{\circ}\text{C}$ ,  $T_g$  is predicted to vary between  $-46$  and  $-52^{\circ}\text{C}$  and hence, the DSC traces obtained both on cooling and heating should, in principle, contain a step in the baseline associated with the change in heat capacity occurring during the glass transition. We have not attempted to superimpose such a baseline on our experimental data and this may account, at least in part, for the discrepancy between the mass of water crystallizing and subsequently melting. The baselines in the DSC experiments do not show a step change either on cooling or heating, strongly suggesting that the change in heat capacity during the glass transition must be small. This implies that the error associated with the assumption of a flat baseline is also small.

At the root of these large discrepancies, between the mass of water crystallizing and subsequently melting, see Table I, may again be the energetically differing types of water in the gel. We have seen already that the crystallization behavior implies that different types of water freeze over a wide temperature range. This will give rise to a range of solid structures. On heating, it is possible that these structures melt and recrystallize prior

to finally melting at ca. 0 °C. These endothermic and exothermic processes can effectively counteract each other over the whole sample and be reflected in an apparently flat baseline. The crystals melting at 0 °C are not, therefore, those that crystallized during cooling but are rather larger and more ordered. Thus, the melting endotherm will be appreciably larger than the sum of the crystallization exotherms. We note, however, that this interpretation brings into question the assumption that the melting enthalpy of water can be used to quantify the peaks observed.

An alternative explanation for the discrepancy between the mass of water crystallizing and subsequently melting, see Fig. 7, allows crystallization to occur during annealing at either – 50 or – 100 °C. This would not be detected by DSC. In the preceding discussion, we noted that the glass transition temperatures of the hydrogels plasticized by the unfrozen water are predicted to be ca. – 50 °C and it has been assumed elsewhere [8] that on vitrification of the gel, no further crystallization of the water can occur. The data listed in Table I show, however, that on increasing the annealing time, the amount of unfrozen water decreases, which strongly suggests that there is sufficient mobility in the glass state for crystallization to occur, albeit on a much slower time-scale. This is presumably water contained in small cavities and whose structure, therefore, deviates significantly from that of the bulk water. Only a small amount of water appears to crystallize during annealing, however, and this alone would not account for the behavior seen in Fig. 7.

Finally, the data shown in Table I clearly reveals that the hydrogel contains water which does not freeze under the experimental conditions. This water amounts to approximately three molecules per repeat unit of the polymer and is consistent with the view that this is water in a hydration shell surrounding the polymer chains. The observation that this water does not freeze presumably indicates that the interaction energy between the water molecules and the hydrophilic segments is greater than the ice nucleation energy.

## 6. Summary

In this study we investigated the interaction of water with pHEMA using a variety of thermal analysis techniques. These techniques were used to show the behavior of hydrated pHEMA (water content 43%) on heating and cooling, as well as the relationship between water content and the glass transition of the gel.

To explain the results from our study, we attempted to use a simple model consisting of a single class of water,

as suggested by previous researchers. However, this model could not account for all our observations. A more satisfactory explanation was found when an alternative model was invoked, consisting of three different classes of water which are in dynamic equilibrium.

Our conclusions are, therefore, that the water in a pHEMA hydrogel is partitioned into the following classes:

1. Hydration water which is in close proximity to the polymer.
2. Interstitial water in regions or cavities surrounded by polymer chains.
3. Bulk water.

## Acknowledgments

We thank the Engineering and Physical Sciences Research Council (UK) for funding this research (grant number GR/M42732/01) and the Medical Research Council for a Senior Fellowship for RMA.

## References

1. V. J. MCBRIERTY, S. J. MARTIN and F. E. KARASZ, *J. Mol. Liq.* **80** (1999) 179.
2. H. B. LEE, M. S. JHON and J. D. ANDRADE, *J. Colloid Interface Sci.* **51** (1975) 225.
3. D. G. PEDLEY and B. J. TIGHE, *Brit. Polym. J.* **11** (1979) 130.
4. H. XU, J. K. VIJ and V. J. MCBRIERTY, *Polymer* **35** (1994) 227.
5. G. SMYTH, F. X. QUINN and V. J. MCBRIERTY, *Macromolecules* **21** (1988) 3198.
6. L. FAMBRI, C. GAVAZZA, M. STOL and C. MIGLIARESI, *Polymer* **34** (1993) 528.
7. L. BOSIO, G. P. JOHARI, M. OUMEZZINE and J. TEIXEIRA, *Chem. Phys. Lett.* **188** (1992) 113.
8. W. E. ROORDA, A. B. JOHANNA, M. A. DE VRIES and H. E. JUNGINGER, *Pharm. Res.* **5** (1988) 722.
9. J. RAULT, A. LUCAS, R. NEFFATI and M. MONLEON PRADAS, *Macromolecules* **30** (1997) 7866.
10. R. WOLFSON and J. M. PASACHOFF. "Physics with Modern Physics for Scientists and Engineers", 2nd edition (HarperCollins College Publishers, New York, 1995) p. 489.
11. W. E. ROORDA, A. B. JOHANNA, M. A. DE VRIES and H. E. JUNGINGER, *Biomaterials* **9** (1988) 494.
12. Y. M. SUN and H. L. LEE, *Polymer* **37** (1996) 3915.
13. J. M. G. COWIE, "Polymers: Chemistry & Physics of Modern Materials", 2nd edition (Blackie, Glasgow, 1991) p. 329.
14. P. JENNISKENS and D. F. BLAKE, *Astrophys. J.* **473** (1996) 1104.
15. Y. MAEDA and H. KITANO, *Spectrochim. Acta. A* **51** (1995) 2433.
16. S. UTOH, *J. Chem. Phys.* **115** (2001) 601.
17. C. A. ANGELL, in "Water, a Comprehensive Treatise", volume 7, edited by F. Franks (Plenum Press, New York, 1982) p. 1.

Received 16 April

and accepted 12 June 2002